NASA TECHNICAL
MEMORANDUM

NASA TM X- 71461

CASE FILE
COPY

MINIMIZING BOUNDARY LAYER BLEED FOR A MIXED COMPRESSION INLET

by Joseph F. Wasserbauer, Robert J. Shaw, and Harvey E. Neumann
Lewis Research Center
Cleveland, Ohio 44135

MINIMIZING BOUNDARY LAYER BLEED FOR A

MIXED COMPRESSION INLET

by Joseph F. Wasserbauer, Robert J. Shaw, and Harvey E. Neumann

Lewis Research Center

ABSTRACT

An experimental investigation of a full scale mixed compression inlet sized for the TF30-P-3 turbofan engine was conducted at Mach 2.5 and 2.0 operating conditions. The two cone axisymmetric inlet had minimum internal contraction consistent with high total pressure recovery and low cowl drag. At Mach 2.5, inlet recovery exceeded 0.90 with only 0.02 centerbody bleed mass-flow ratio and zero cowl bleed. A centerbody bleed of approximately 0.05 gave a maximum inlet unstart angle-of-attack of 6.85°. Inlet performance and angle-of-attack tolerance is presented for operation at Mach 2.5 and 2.0.

INTRODUCTION

Supersonic inlets should be able to operate efficiently with low drag over the entire flight range of the aircraft. For flight speeds above Mach 2.0, mixed-compression inlets offer this capability. However, some means of varying the inlet's contraction ratio must be provided to supply engine airflow demands at flight speeds below Mach 2.0.

Two-dimensional inlets provide variation of contraction ratio by relatively simple movable ramp surfaces. The problem is more difficult with axisymmetric designs. Single cone axisymmetric inlets have been designed which vary the contraction ratio by either collapsing or translating the centerbody, or by collapsing the cowl and translating the centerbody, references 1 and 2. In general, these single cone axisymmetric inlets have high internal contraction which result in a fairly long supersonic diffuser. Consequently a relatively high boundary layer bleed flow rate is necessary to provide the desired inlet performance at design flight speeds.

An inlet designed with less internal contraction would perform with less bleed drag. Although a possible increase in cowl pressure drag may nullify this improvement in bleed drag, other desirable characteristics (such as improved angle-of-attack tolerance) may be established for certain mission applications.

In reference 3, an inlet, with less internal contraction and shortened supersonic diffuser, showed reductions in performance bleed while maintaining relatively high pressure recovery. In addition, significant increases in angle-of-attack tolerance were also demonstrated. The inlet of reference 3 and the inlet presented here-in used similar design philosophies. This inlet design used a two-cone spike to provide the maximum external compression compatible with high total-pressure recovery with relatively low cowl drag. The overall length from the cowl lip to inlet throat was kept short to minimize bleed flow requirements. Boundary layer calculations indicated a small displacement thickness at the throat. Vortex generators were used in the subsonic diffuser to reenergize the boundary layer. For a flight inlet, the second-cone would be collapsed to vary contraction ratio and at its lowest position would blend into the first-cone contours so as to provide a single cone centerbody. The design provided 47.5 percent of the supersonic area contraction internally for a design Mach number of 2.5.

The objectives of this study were, (1) the development of an axisymmetric mixed-compression inlet based on the aforementioned philosophy, and (2) to demonstrate that the performance bleed could be reduced from previous experimental minimum values by reducing supersonic diffuser length while maintaining good inlet performance. Various cowl and centerbody bleed configurations were investigated to determine the minimum bleed and its effect on performance. The performance of the final inlet configuration with the minimum bleed is presented in this paper.

The inlet, coupled to a cold pipe-choked plug assembly, was tested at Mach numbers of 2.5 and 2.0. Inlet flow surveys were made at the inlet throat and throat exit station, midway in the subsonic diffuser, and at the diffuser exit to evaluate local flow conditions. In addition to the flow surveys, measurements were made of the centerbody bleed flow rates,

total-pressure recovery, and engine face distortion. The maximum angle-of-attack before an inlet unstart was determined for peak, critical, and supercritical inlet operation. The effect of an overload bypass system was also evaluated.

APPARATUS AND PROCEDURE

The inlet of this investigation was designed for operation at a free-stream Mach number of 2.5. It is a full scale design, sized to match the air flow requirements of the TF30-P-3 turbofan engine. An isometric view of the inlet and its installation in the 10- by 10- foot supersonic wind tunnel is shown in figure 1.

The internal contous of the supersonic diffuser were determined with the method of characteristics flow solution described in reference 4. Details of the inlet are presented in the cross section view in figure 2. At the design Mach number of 2.5 the centerbody cone angles are 12.5^O for the initial cone angle and 18.5^O for the second-cone angle, figure 2(a). To minimize costs of this particular inlet model, the spike did not collapse but rather was translated to vary the internal contraction ratio during testing. Hence, a second centerbody was designed as a collapsed version for Mach 2.0 operation. Its initial cone angle was 12.5^O and the second-cone angle was 14.5^O. The inlet cowl lip was sharp and the initial internal cowl angle was 2^O. The external cowl angle was kept at 5° to minimize cowl drag.

The inlet design was such that the isentropic compression fan from the cowl and the cowl-lip oblique shock were nearly focused on the centerbody, figure 2(b). The cowl-lip shock and cowl compression fan were cancelled at the centerbody with a sharp turn and short length of contoured surface before the throat as prescirbed by the inlet design computer program. A centerbody bleed slot replaced the short length of contoured surface over this compression region for boundary layer control ahead of the inlet throat.

In reference 3, the cowl shock and cowl compression fan were focused at one point on the centerbody. An abrupt turn on the centerbody was

used to cancel reflected shocks. A flush slot bleed was positioned ahead of this focal point at the end of the second cone contour. The local flow expansions from the slot and the large static pressure rise on the center-body, caused by the focused shock-compression fan system, gave less than desired control of the boundary layer at this point. By positioning the bleed slot behind the cowl shock impingement point, advantage could be taken of the higher surface static pressures to provide better bleed pumping char-acteristics and higher bleed pressure recoveries in the centerbody cavity. Because of the better bleed pumping characteristics, local boundary layer separations in this region could be minimized. For this inlet design, the slot spans the length of compression fan impingement region, 0.053 cowl-lip diameters. A blunt leading edge and the flush slot arrangement proved to be the most efficient slot geometry during a centerbody bleed evaluation study.

The slot bleed permits a relatively simple geometry to be retained during collapse of the centerbody. The relatively high pressure on the 18.5° second cone tends to relieve recirculation problems due to possible leakage on the collapsable surface. The focused compression reduces significantly the supersonic diffuser length from cowl lip to inlet throat, (0.38 cowl-lip diameter), and thus reduces the amount of cowl bleed, if any, that may be required at the inlet throat. Regions of cowl bleed were provided at the inlet throat. The cowl bleed evaluation study showed that the increased performance did not offset the increased cowl bleed drag for all configurations tested. Therefore, these bleed regions were sealed for the data presented here-in.

The centerbody bleed flow was ducted to four equally spaced support struts located over half of the subsonic diffuser length. The centerbody bleed flow is controlled by a butterfly valve in each strut. The centerbody duct and strut system was designed to pass approximately 6 percent of the capture mass flow ratio. The theoretical pressure recovery in the inlet throat ahead of the terminal shock-wave system was 98 percent with a throat Mach number of about 1.3.

A one dimensional analysis was used to design the subsonic diffuser. A diffuser length of 1.5 inlet diameters was selected. The diffusion area

ratio was matched to the compressor face Mach number required for the TF30-P-3 turbofan engine at Mach 2.5 operation. This resulted in an equivalent conical diffusion angle of 10° for the subsonic diffuser. Vortex generators were used on the cowl and centerbody to inhibit flow separation.

The internal flow area distributions for the Mach 2.5 and 2.0 centerbodies are shown in figure 3. An attempt was made to base the distributions of the subsonic diffusers on a linear pressure variation. But the geometry of the inlet struts modified the area distribution such that the linear pressure variation of the diffuser was compromised. The effect is more pronounced for the Mach 2.0 centerbody design.

The inlet was also equipped with eight overboard bypass doors designed for high frequency control studies, reference 5. The doors were slotted plates which were hydraulically actuated. A detailed description of the bypass doors is presented in reference 6. The diffuser bypass flow passed through the choked slotted plate to a plenum and then through a louvered panel to the free stream.

The inlet was tested with and without an operating inlet bypass system. When bypass doors were not used, insert blanks replaced the bypass door assemblies so that smooth surfaces were maintained on the cowl from the cowl lip to the diffuser exit.

The inlet flow was surveyed at the throat, throat exit, midway in the subsonic diffuser, and at the diffuser exit. The diffuser exit plane was surveyed by 12 total pressure rakes of 6 area weighted tubes per rake. Three rakes at 0°, 90°, and 180° had additional tubes at the hub and tip to survey the boundary layer. Three dynamic total pressure probes were used to sample RMS values of pressure at the diffuser exit. Their locations are shown in the sketch in figure 2(a).

RESULTS AND DISCUSSION

The inlet performance for Mach 2.5 and 2.0 operation without an operating bypass system is shown in figure 4. The variation of pressure recovery with inlet bleed mass flow ratio, steady-state distortion, and

dynamic distortion is presented. The steady state distortion is defined as the maximum minus the minimum total pressure divided by the average total pressure. An average RMS value of the fluctuating component of the total pressure was obtained for three dynamic probes. Dynamic distortion is defined as this average divided by the average total pressure. The variation of bleed flow over the inlet operating range is emphasized by the presentation of the inlet bleed mass flow ratio. The inlet of this investigation was designed to spill 0.5% of the inlet capture mass flow at Mach 2.5 operation. The engine mass flow ratio is then the inlet capture mass flow ratio, 0.995, minus the inlet bleed flow.

At the design free stream Mach number of 2.5, peak pressure recovery was 0.905 at a bleed mass flow ratio of only 0.021. The centerbody bleed exit area was maintained constant for all data with open symbols in figure 4. For critical and supercritical operation, the bleed mass flow ratio was 0.019. Critical operation is defined herein as the terminal shock positioned at the inlet geometric throat and supercritical operation as the terminal shock downstream of the inlet throat. In this report, results pertain only to started inlet operation. Hence, subcritical operating points refer to a terminal shock position just upstream of the geometric throat in the region of the bleed slot.

The potential stable subcritical operating range of the inlet is indicated by the solid symbols in figure 4. The inlet bleed mass flow ratio was varied by changing the bleed exit area via the strut butterfly valves. With the maximum bleed exit area available, 5% of the inlet capture mass flow ratio was removed before the inlet unstarted. The peak inlet pressure recovery during this subcritical operation was 0.915.

Steady state distortion varied from about 8% to 11% when the inlet was operated from critical to supercritical operation. For subcritical operation, steady state distortion varied from 6 to 8%. Dynamic distortion remained about 2 percent over the range of inlet operation. However, it must be noted that the dynamic activity was measured at only three total pressure probe locations at the diffuser exit plane, (see figure 2(a)). The dynamic activity over the remainder of the diffuser exit plane was to be measured in a subsequent test. In general, the level of dynamic

activity appears to be acceptable for operation at the Mach 2.5 condition.

Inlet performance for the collapsed version of the centerbody at Mach 2.0 is shown in figure 4(b). Peak inlet performance for the fixed bleed exit area was 0.940 with only 0.014 bleed mass flow ratio. Inlet capture mass flow ratio at Mach 2.0 was 0.918 and the remainder was spilled around the cowl through the spike shock systems. Variation of the bleed exit area increased the bleed mass flow ratio to 0.045 and provides a measure of inlet stability at this Mach number. Steady state distortion varied from 8% to 12%, a slight increase, while dynamic distortion dropped to about 1.0 percent over the range of inlet operation at Mach 2.0.

Distributions of local recovery profiles are shown in figure 5 for Mach 2.5 critical operation and in figure 6 for Mach 2.0 critical operation. These profiles are presented for the throat, throat exit, mid diffuser, and diffuser exit locations. The individual tube pressures at the throat station are uncorrected and represent the measured pressure behind a normal shock.

At the Mach 2.5 operation, the cowl surface Mach number diffuses from 1.8 to 1.3. Figure 5 shows the normal shock recoveries near the cowl at the throat station correspond to the predicted value of 0.96. Because of the short cowl length from the lip to throat, the boundary layer growth appears to be moderate at the throat. The incompressible shape factor of the measured cowl boundary layer was about 1.45. This indicates that the flow in the boundary layer was not near separation, (a shape factor of about 1.8 would indicate boundary layer separation problems). Further, the measured displacement thickness was in good agreement with analytical predictions. Therefore, it confirms the design philosophy that by shortening the supersonic diffuser, minimization of the cowl bleed can result.

The centerbody throat rake was positioned slightly ahead of the inlet throat. The centerbody bleed slot was located just ahead of this rake, (see figure 2(a)). The lower measured local pressure recoveries at this rake station could be a result of local flow expansion due to the bleed slot.

Comparison of the throat exit and mid-diffuser profiles near the centerbody indicate that the vortex generators energized the flow. At the

diffuser exit, low distortion profiles were measured. It appears that the vortex generators minimized any potential flow problems that might have occurred.

At Mach 2.0 operation, (see figure 6), the throat and throat exit profiles appear well behaved. The flow profiles at the mid-diffuser and compressor face show higher flow distortions than those measured for Mach 2.5 operation. This is attributed to the adverse area variation through the strut region as was indicated in figure 3.

At Mach 2.5 operation, the 4 percent loss in total pressure in the supersonic diffuser matched the theoretical predictions. The overall loss in pressure recovery was 10 percent. Of this loss 6 percent occurred in the subsonic diffuser. At Mach 2.0 operation, the overall loss in pressure recovery was only 6 percent. Potential improvements in the subsonic diffuser to minimize pressure recovery loss and distortion are possible by redesign of the inlet struts and recontouring the subsonic diffuser.

Overall inlet performance at Mach 2.5 with an operating bypass system is shown in figure 7. With a constant centerbody bleed mass flow ratio of 0.02, the peak pressure recovery was 0.894. This is about 0.01 less than the pressure recovery for inlet operation without bypass flow. For the maximum centerbody bleed, the peak pressure recovery increases to 0.911. Near critical inlet operation, the data indicate a steady state distortion 2 percent higher than that measured without the bypass system. Dynamic distortion, on the other hand, remained about the same.

Comparison of the total pressure rake profiles at critical inlet operation for bypass and no bypass flow is shown in figure 8. Only one quadrant is shown, but was representative of the other quadrants because of symmetry. A comparison shows that the center rake profile (rake 1) was essentially the same for either inlet operation. However, the two side rakes, rake 12 and rake 2, in figure 8(a), show tendancies to separate on the cowl when the bypass was operating. The result was a reduction in pressure recovery and increase in steady state distortion when the inlet bypass system was operating.

Rakes, such as rake 12 and rake 2, measure the flow over the bypass door entrance slots. The entrance slots cover about the last one third of the diffuser length and are in the rapid diffuser area variation region. The depletion of the duct mass flow through the bypass doors has the effect of increasing the slope of the diffuser area variation and causing a more adverse pressure gradient on the cowl. This would tend to separate the flow, at least locally, as indicated by the comparison.

A comparison of diffuser exit contour maps for bypass and no bypass flow at critical inlet operation is presented in figure 9. The contour maps are a result of a computer program which uses the total pressure inputs at the diffuser exit but does not include the effect of the inlet support struts. The solid lines on the contour plots show the position of the struts. The numerical values indicated in figure 9 represent the average recovery for each of the shaded regions. These plots show that there is little circumferential distortion content and that most of the distortion is radial for both cases. However, with the overboard bypass operating, figure 9(a) shows a lower pressure recovery region in the vicinity of the struts. This is a result of the reduction in pressure recovery mear the cowl in the vicinity of the bypass doors as previously shown in figure 8(a).

Inlet performance over an angle-of-attack range is shown in figure 10. The overboard bypass system was operating for these data. The angle-of-attack operation is presented for both minimum and maximum centerbody bleed exit areas. At a constant centerbody bleed, mass flow ratio of 0.021, the maximum angle-of-attack was 2.55°. For critical inlet operation, that is with the terminal shock in the throat, the angle-of-attack before an inlet unstart was 1.74°. This was increased to 4.17° by increasing centerbody bleed which relieves overcompression in the throat region due to angle-of-attack operation. The maximum unstart angle-of-attack that was attained during supercritical operation was 6.85°. To obtain this angle, the full capacity of the centerbody bleed system was employed.

Steady state distortion at an angle-of-attack of 4.17° was 0.196 and at an angle-of-attack of 6.85° was 0.305. Although the inlet demonstrated a relatively large angle-of-attack range when using the increased center-

body bleed, distortion may be a limiting factor. Consideration of the useful angle-of-attack range of any inlet must include the distortion sensitivity of the particular engine to which it is coupled.

Tolerance of turbofan and turbojet engines to inlet generated total pressure distortion depends on the spatial distribution of the distortion. Circumferential distortions are usually more difficult for an engine to accept then radial distortions. Both the amplitude and extent of a circumferential distortion are of importance. Recent tests, reference 7, have indicated that the TF30 engine is sensitive to angular extents of 180°. This type of distortion is generally obtained in axisymmetric inlets at angle-of-attack.

Figure 11 shows the compressor face contours maps for the various angle-of-attack data presented in figure 10. For low angles-of-attack, up to about 2°, the distortion appears to be more radial than circumferential. The circumferential distortion increases as the angle-of-attack is increased beyond 2°. Because of the increasing circumferential distortion and depending on the type of engine employed, it appears then, that the limiting angle-of-attack lies between 2° and 6.85°. However, unpublished results from a subsequent test using this inlet with the TF30-P-3 engine indicate that the complete range of angle-of-attack is potentially useful.

The stability performance and bleed characteristics of the centerbody bleed system are presented in figure 12. The various symbols represent given constant bleed exit areas. The dashed curves were generated by reducing the compressor face airflow from the critical value, causing the terminal shock to move forward of the inlet throat into the bleed slot until unstart occurred. At a given bleed exit area, the bleed mass flow ratio is constant for supercritical operation.

The stability characteristics of the bleed system would be used only when some inlet flow disturbance would cause the terminal shock to move forward of the throat and unstart the inlet. Some control scheme would be needed which employs the full capacity of the bleed system.

For simplicity, an active control appears to be a feasible design. This control would provide full bleed exit area and maximum bleed mass

flow ratio upon command from some control parameter, such as step changes in throat Mach number.

The inlet tested here demonstrated some inlet stability margin by use of only a centerbody bleed system. In reference 8, a cowl stability bleed system was demonstrated that would not be activated unless the terminal shock moved forward of the inlet throat. Use of this cowl stability system coupled with the inlet centerbody bleed system should provide adequate inlet stability for most inlet disturbances while maintaining the inlet minimum bleed characteristics during normal operation.

CONCLUDING REMARKS

A design concept for high performing supersonic mixed compression inlets is examined that would provide maximum external compression and maintain good performance. This permits short supersonic diffusers with short cowl lengths that generate a thin boundary layer and eliminate the need for cowl bleed. Based on this design concept an experimental investigation was conducted to evaluate the performance of a full scale axisymmetric mixed compression inlet. The inlet was designed to provide airflow for a TF30-P-3 engine at Mach number of 2.5. A slot bleed was used on the centerbody and provides a simple geometry for a collapsing centerbody. The 18.5° second-cone provides relatively high pressure on the cone surface to minimize recirculation. The following results were obtained:

1. At Mach 2.5 for inlet operation without bypass, the inlet pressure recovery exceeded 0.90 with only 0.02 centerbody bleed mass flow ratio and zero cowl bleed. Hence, it compares favorably with similar high performance inlets which have lower cowl drag but greater bleed drag. Variation of the centerbody bleed exit area provides additional stability range for subcritical operation. At Mach 2.0 the inlet total pressure recovery was 0.94 with only 0.015 centerbody bleed mass flow ratio.

2. At Mach 2.5 operation and with the minimum centerbody bleed mass flow ratio of 0.02, the maximum inlet unstart angle-of-attack operation for the inlet was 2.55°. Increasing the centerbody bleed mass

flow ratio to approximately 0.05 gave maximum inlet unstart angle-of-attack of 6.85°.

3. Inlet steady state distortions varied from 6 percent to 11 percent for Mach 2.5 and from 8 percent to about 12 percent for Mach 2.0 operation for inlet operation without bypass.
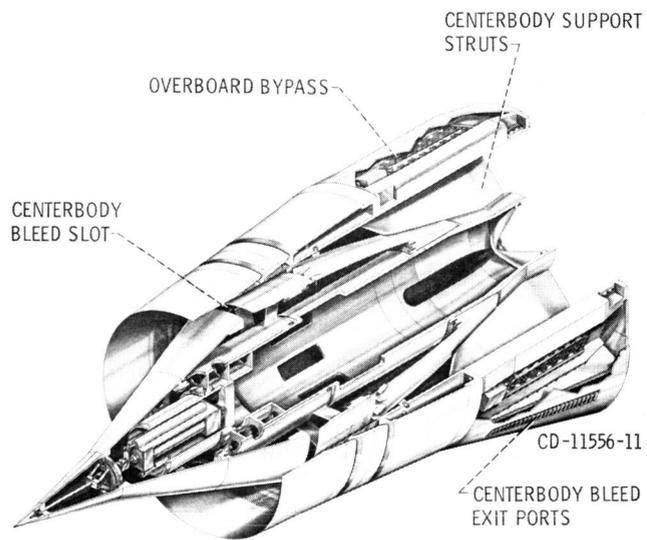
4. Diffuser toal pressure profiles on the cowl at the inlet throat and throat exit stations show acceptable boundary layer profiles at the various operating conditions without the benefit of cowl bleed. The 4 percent loss in total pressure in the supersonic diffuser matched the theoretical predictions.

5. The overall loss in total pressure recovery was 10 percent. Of this loss, 6 percent occurred in the subsonic diffuser. Inlet operation with an operating bypass system also reduced the total pressure recovery slightly and increased the steady state distortion. Potential improvements in the subsonic diffuser to minimize pressure recovery loss and distortion are possible by redesign of the inlet struts and bypass system and recontouring the subsonic diffuser.
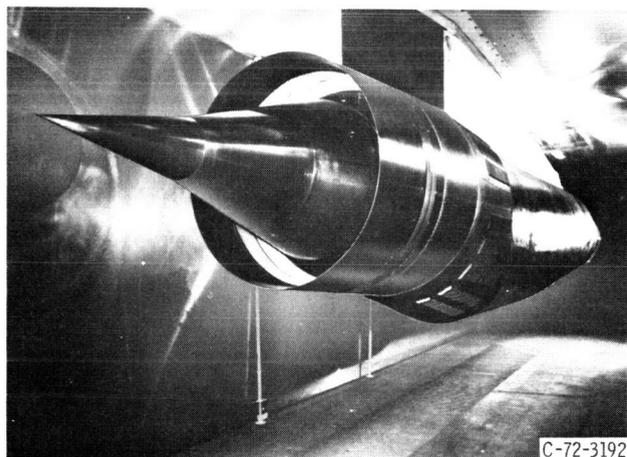
REFERENCES

1. Smeltzer, D.B., and Sorensen, N.E., "Tests of a Mixed Compression Axisymmetric Inlet With Large Transonic Mass Flow at Mach Numbers 0.6 to 2.65", TN D-6971, 1972, NASA, Moffett Field, Calif.

2. Koncsek, J.L., and Syberg, J., "Transonic and Supersonic Test of a Mach 2.65 Mixed-Compression Axisymmetric Intake", CR-1977, 1972, NASA, Washington, D.C.

3. Wasserbauer, J.F., and Choby, D.A., "Mach 2.5 Performance of a Bicone Inlet With Internal Focused Compression and 40 Percent Internal Contraction", TM X-2294, 1971, NASA, Cleveland, Ohio.

4. Anderson, B.H., "Design of Supersonic Inlets by a Computer Program Incorporating the Method of Characteristics," TN D-4960, 1969, NASA, Cleveland, Ohio.

5. Baumbick, R. J., Wallhagen, R. E., Neiner, G. H., and Batterton, P. G., "Dynamic Response of Mach 2.5 Axisymmetric Inlet With 40 Percent Supersonic Internal Area Contraction", TM X-2833, 1973, NASA, Cleveland, Ohio.

6. Webb, J. A., Jr., Mehmad, O., and Hiller, K. W., "Improved Design of a High-Response Slotted-Plate Overboard Bypass Valve for Supersonic Inlets", TM X-2812, 1973, NASA, Cleveland, Ohio.

7. Werner, R. A., Abdelwahab, M., and Braithwaite, W. M., "Performance and Stall Limits of an Afterburner-Equipped Turbofan Engine With and Without Inlet Flow Distortion", TM X-1947, 1970, NASA, Cleveland, Ohio.

8. Sanders, B. W. and Mitchell, G. A., "Increasing the Stable Operating Range of a Mach 2.5 Inlet", Paper 70-686, June 1970, AIAA, New York, N. Y.

CENTERBODY SUPPORT
STRUTS

OVERBOARD BYPASS

CENTERBODY
BLEED SLOT

CD-11556-11

CENTERBODY BLEED
EXIT PORTS

(a) ISOMETRIC VIEW OF MODEL.

C-72-3192

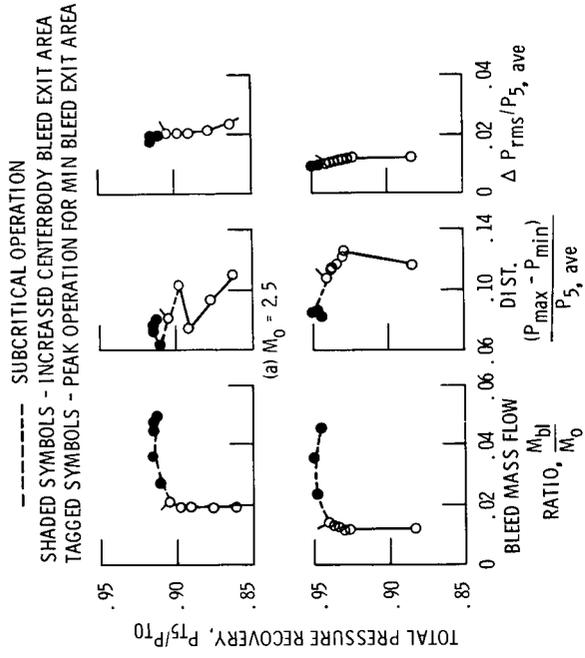(b) INSTALLATION IN 10- BY 10-FOOT SUPERSONIC WIND TUNNEL.

Figure 1. - Mach 2.5 Inlet.

SUBCRITICAL OPERATION

SHADED SYMBOLS - INCREASED CENTERBODY BLEED EXIT AREA
TAGGED SYMBOLS - PEAK OPERATION FOR MIN BLEED EXIT AREA

(a) $M_0 = 2.5$

(b) $M_0 = 2.0$

BLEED MASS FLOW RATIO, $\frac{M_{bl}}{M_0}$

$\frac{(P_{max} - P_{min})}{P_5, ave}$

$\Delta P_{rms}/P_5$, ave

TOTAL PRESSURE RECOVERY, P_{t5}/P_{t0}

Figure 4. - Inlet performance. No bypass flow.

$M_0 = 2.0$ DESIGN

$M_0 = 2.5$ DESIGN

DIFFUSER STATION, x/R, COWL-LIP-RADII

DIFFUSER FLOW AREA RATIO, A/A_c

Figure 3. - Area variation.

STATION:
AXIAL DISTANCE x/R_c

0   1   2   3   4   5
   2.015 2.837 3.212 4.604 5.607

OVERBOARD BYPASS

18.5°

12.5°

5° 2°

VORTEX GENERATORS

CENTERBODY BLEED CAVITY

RMS PROBES

STRUTS

INLET RAKES
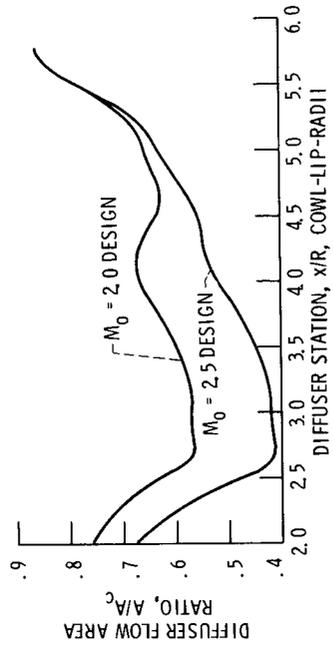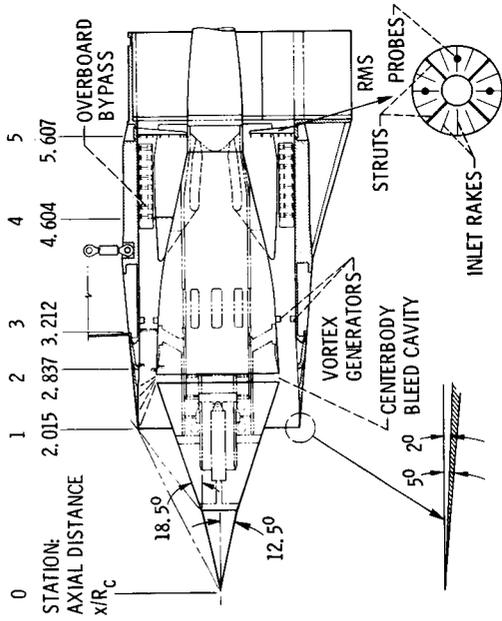
(a) INLET CROSS SECTION AND DIFFUSER INSTRUMENTATION.

0.38 COWL LIP DIAMETERS

INITIAL CONE SHOCK

SECOND CONE SHOCK

COWL SHOCK

SECOND CONE

18.5°

GEOMETRIC THROAT

COWL ISENTROPIC COMPRESSION FAN

0.053 COWL LIP DIAMETERS

CENTERBODY BLEED SLOT
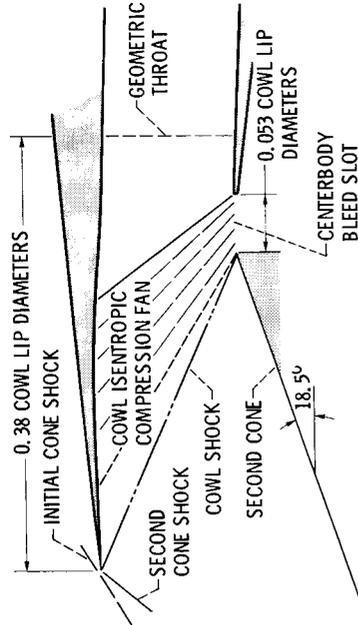
(b) SUPERSONIC DIFFUSER DETAILS.

Figure 2. - Inlet details.

COM-
PRES-
SOR
FACE

THROAT
EXIT

MID-
DIFFUSER

THROAT

PERCENT OF LOCAL DUCT HEIGHT, h/H

LOCAL TOTAL PITOT PRESSURE, P_T/P_{T_0}
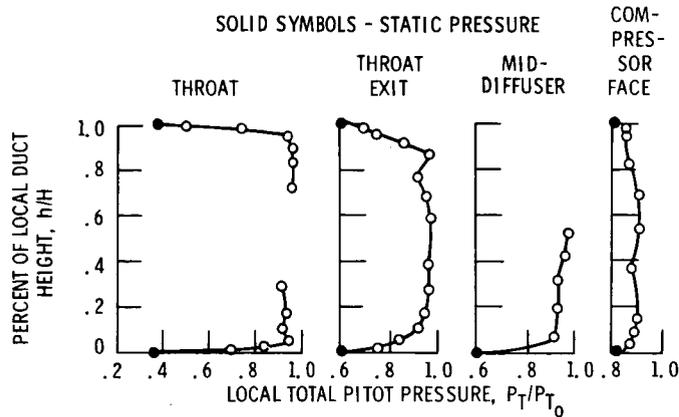
Figure 5. – Diffuser performance, $M_0 = 2.5$, critical inlet operation, $M_{bl}/M_0 = .019$.

SOLID SYMBOLS – STATIC PRESSURE

THROAT
EXIT

MID-
DIFFUSER

COMPRES-
SOR FACE

THROAT

PERCENT OF LOCAL DUCT HEIGHT, h/H

LOCAL TOTAL PITOT PRESSURE, P_T/P_{T_0}
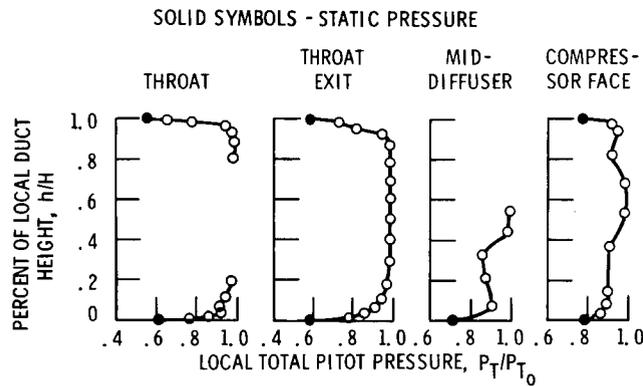
Figure 6. – Diffuser performance, $M_0 = 2.0$, critical inlet operation, $M_{bl}/M_0 = .015$.

－－－－ SUBCRITICAL OPERATION
○ CONSTANT BYPASS DOOR EXIT AREA
□ BYPASS DOOR EXIT AREA VARIATION

TAILED SYMBOLS – PEAK OPERATION, MINIMUM BLEED
EXIT AREA

SHADED SYMBOLS – INCREASED BLEED EXIT AREA

TOTAL PRESSURE RECOVERY, $\dfrac{P_{5, \text{ave}}}{P_0}$

ENGINE MASS-FLOW RATIO, $\dfrac{m_5}{m_0}$

STEADY-STATE DIS-
TORTION

$\dfrac{P_{max} - P_{min}}{P_{5, \text{ave}}}$

DYNAMIC DISTORTION

$\dfrac{\Delta P_{rms}}{P_{5, \text{ave}}}$
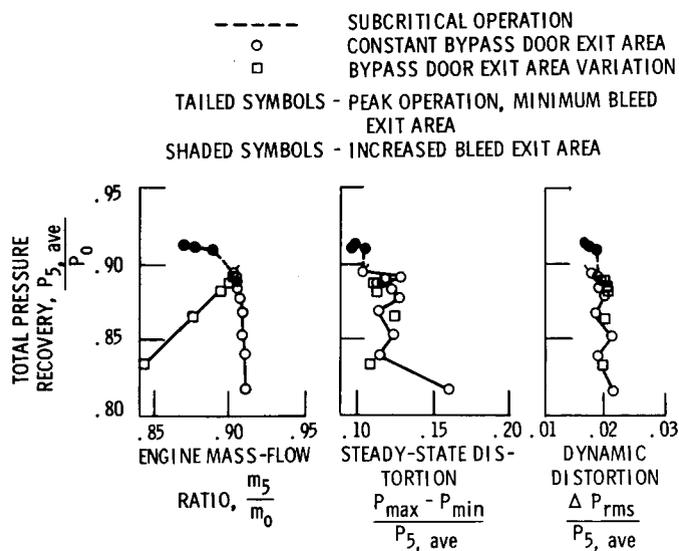
Figure 7. – Inlet performance with bypass flow. $M_0 = 2.5$, $\alpha = 0^0$, $m_{by}/m_0 = .067$.

(a) OVERBOARD BYPASS

(b) NO OVERBOARD BYPASS

LOCAL TOTAL PRESSURE RECOVERY, $\bar{P}/P_0$.

DUCT HEIGHT RATIO, d/H
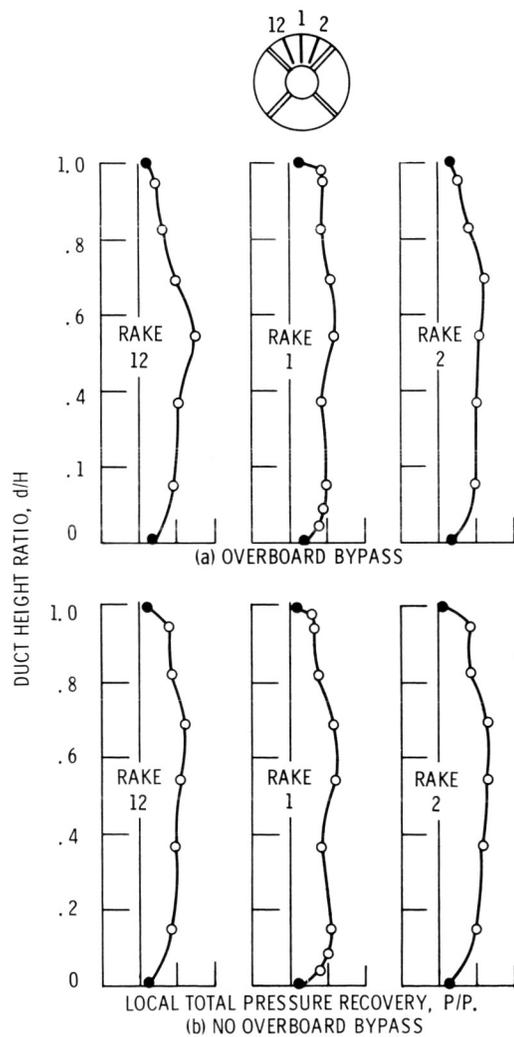
Figure 8. - Typical diffuser exit rake profiles for $\alpha = 0^0$.
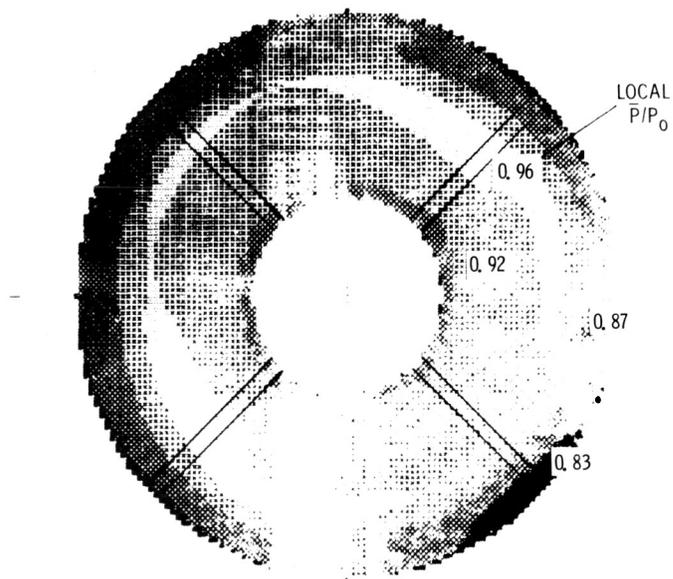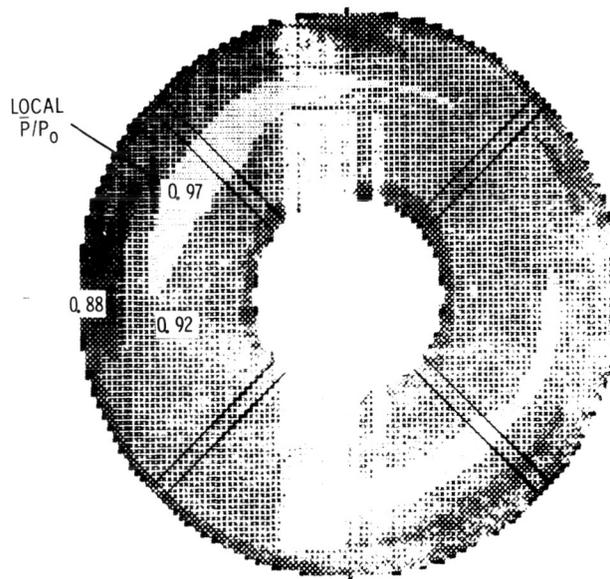
(a) BYPASS FLOW

(b) NO BYPASS FLOW

Figure 9. - Steady-state distortion contours. Critical inlet operation, 0^0 angle of attack, $M_0 = 2.5$.

○ $\alpha = 0^0$
□ α FOR PEAK INLET OPERATION
◇ α FOR CRITICAL INLET OPERATION
△ α FOR SUPERCRITICAL INLET OPERATION

OPEN SYMBOLS - OPTIMUM
   CENTERBODY BLEED EXIT
   AREA
SOLID SYMBOLS - MAX.
   CENTERBODY BLEED EXIT
   AREA

DIFFUSER EXIT MASS FLOW RATIO, $\frac{m_5}{m_0}$

CENTERBODY BLEED MASS FLOW RATIO, M_{bl}/M_0

DISTORTION, $\dfrac{P_{max} - P_{min}}{P_{5,\ ave}}$

TOTAL PRESSURE RECOVERY, P_{T5}/P_{T_0}
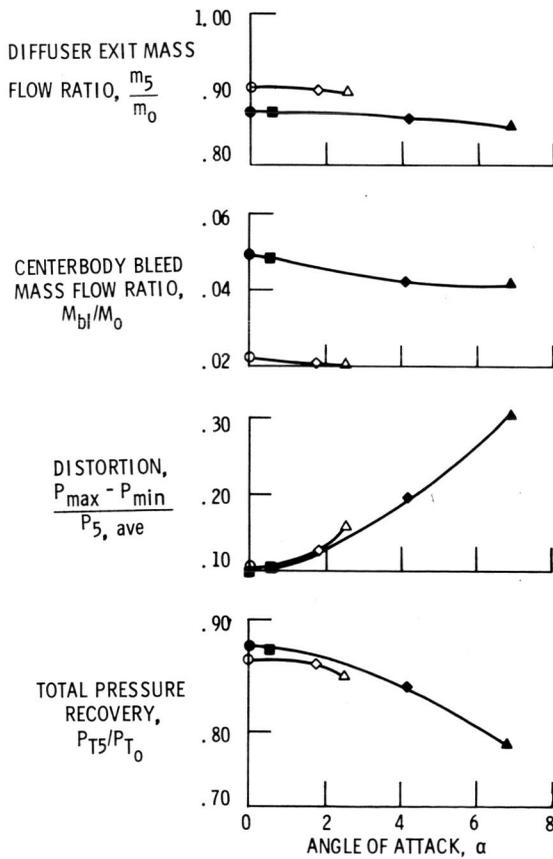
ANGLE OF ATTACK, α

Figure 10. - Inlet angle of attack performance. Inlet overboard bypass operating. $M_0 = 2.5$, $\alpha = 0^0$.

LOCAL $\bar{P}/P_0$

0.93   0.97
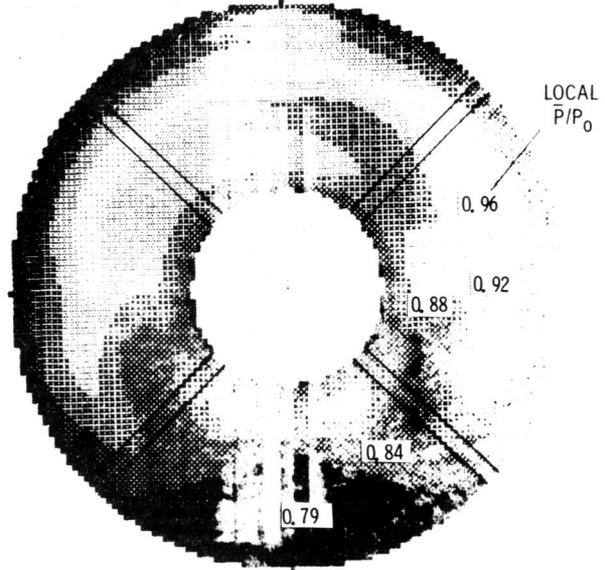
0.88

(a) $\alpha = 0^0$

LOCAL $\bar{P}/P_0$

0.89

0.93

0.98

(b) $\alpha = 0.58^0$
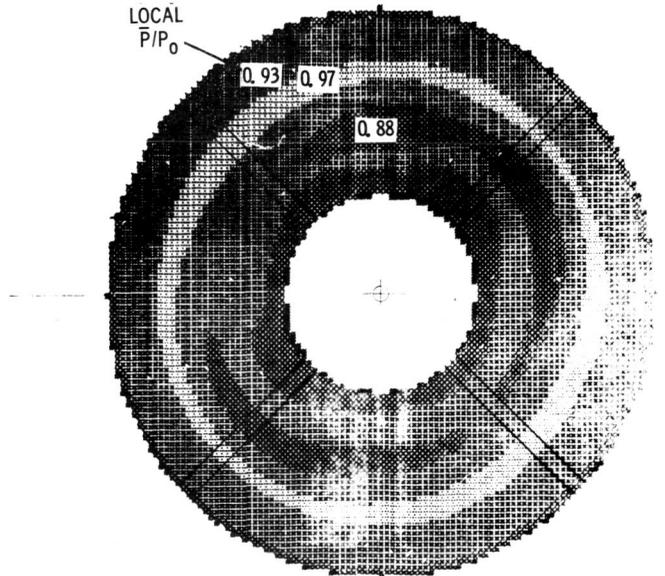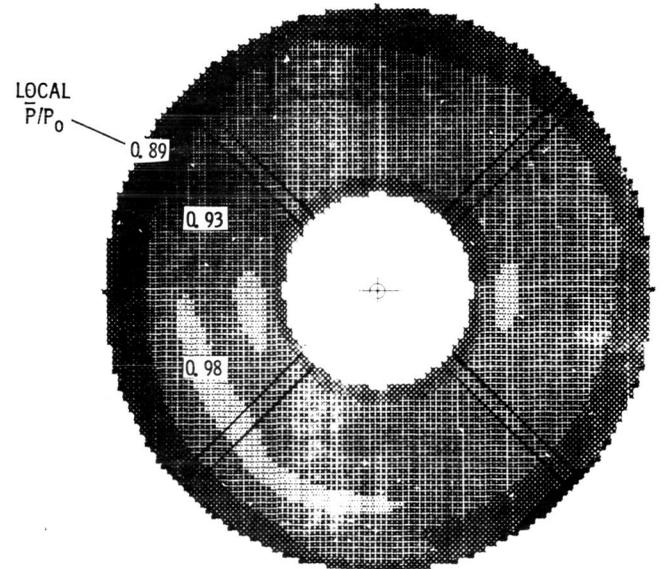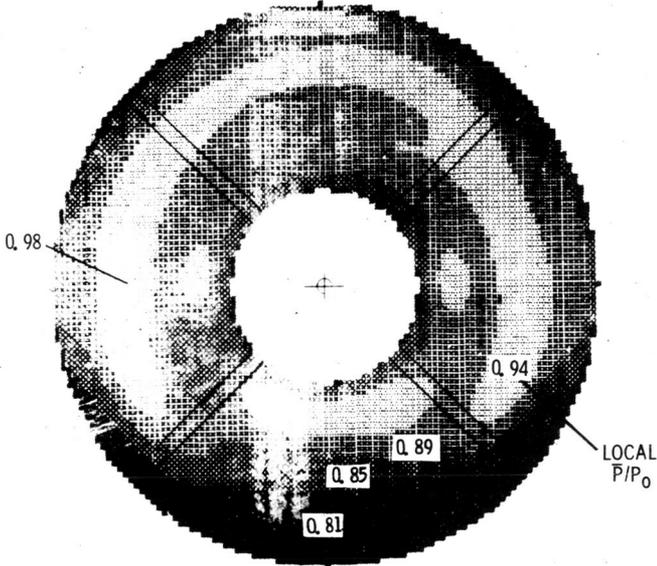
Figure 11. - Steady-state distortion contours. Angle of attack operation. Inlet bypass operating, $M_0 = 2.5$.
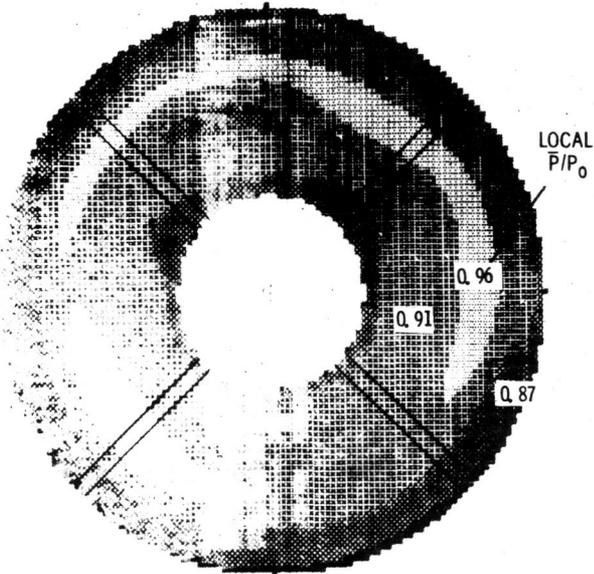
LOCAL
$\bar{P}/P_0$
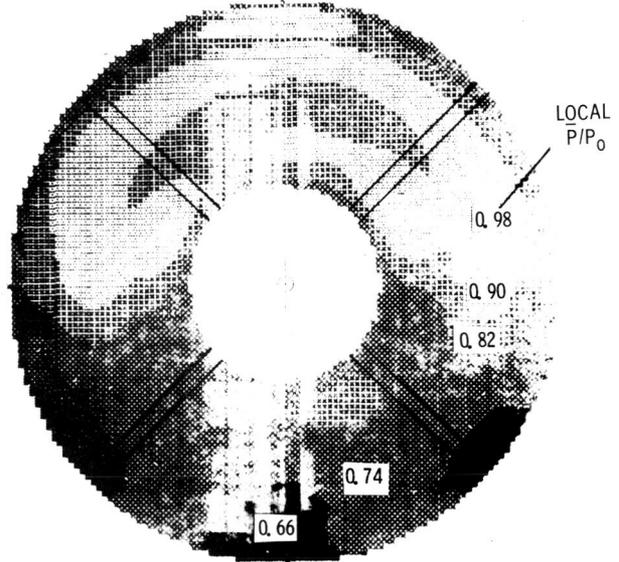
0.96
0.91
0.87

(c) α = 1.78°

LOCAL
$\bar{P}/P_0$

0.96
0.92
0.88
0.84
0.79

(e) α = 4.17°

LOCAL
$\bar{P}/P_0$

0.98
0.94
0.89
0.85
0.81

(d) α = 2.55°

Figure 11. - Continued.

LOCAL
$\bar{P}/P_0$

0.98
0.90
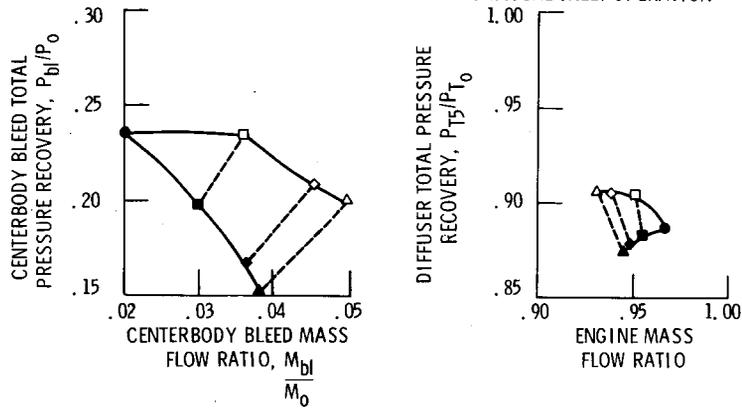0.82
0.74
0.66

(f) α = 6.85°

Figure 11. - Concluded.

Figure 12. – Stability performance at $M_0 = 2.5$ with bypass flow, $M_{by}/M_0 = .01$.